



A Preliminary Study of the Numerical Simulation of a Gaseous Anthracene Compound in an Atmospheric Plasma Reactor for Treating Cooking Fumes

Hung-Chang Chang¹ and Lien-Te Hsieh^{1,2*}

¹ Department of Environmental Engineering and Science, National Pingtung University of Science and Technology, No. 1, Shuefu Road, Neipu, Pingtung 91201, Taiwan.

² Department of Environmental Engineering and Science, National Pingtung University of Science and Technology, No. 1, Shuefu Road, Neipu, Pingtung 91201, Taiwan.

*e-mail: Lthsieh@mail.npust.edu.tw

Abstract

United States Environmental Protection Agency (USEPA) ranked Anthracene (Ant) sixteenth among polycyclic aromatic hydrocarbons (PAHs) priority air pollutants. Computational fluid dynamics (CFD) can be employed to combine knowledge from experiments and theoretical studies by developing chemistry and physics models and evaluating their predictions. Non-uniformity in atmospheric plasma reactor (APR) environments, including flow, temperature, and contaminant concentration distributions, must be considered to optimize design. This can be achieved by applying a CFD technique to an APR for treating cooking fumes through environmental numerical simulation. In simulation, the dimensions and operative conditions of an atmospheric plasma reactor are same as the reactor developed in this study. The reaction zone of the APR was constructed and meshed using a Gambit version 2.4.6 preprocessor. A three-dimensional structured grid comprising approximately 493,000 cells was employed to describe a quarter of the total volume. The commercial CFD program ANSYS Fluent version 12.1 was used to simulate the combustion process in the APR. The Navier–Stokes governing equations were discretized by a finite volume method and flow fields were estimated using the Reynolds Averaged Navier–Stokes (RANS) model. The Eddy-Dissipation Concept (EDC) function was selected to predict air flow temperature distribution and gaseous anthracene compound mass fraction. Results of the preliminary study of numerical simulations showed that the numerical simulated average temperature and Anthracene compound mass fraction in the tail exhaust varied within $\pm 5\%$ of the measured data.

Keywords: Cooking Fume, Atmospheric Plasma, Anthracene, Computational Fluid Dynamics (CFD), Air toxic

1. Introduction

Polycyclic aromatic hydrocarbons (PAHs) are globally distributed environmental contaminants with issues related to their known toxic and bioaccumulative characteristics [1]. In humans for instance, health risks associated with PAHs exposure include cancer and DNA damage. Previous studies reported that cooking fumes contain many kinds of hydrocarbons, such as PAHs, alkanes, alkanolic acids, and alkyl aldehydes. It has been proven that some PAHs are carcinogenic and mutagenic to the human body. Among all PAHs, benzo(a)pyrene (BaP) is the most carcinogenic, which contents account for 1~20% of all carcinogenic PAHs [2-4]. According to the major toxic organic compounds listed by the U.S.EPA (U.S. Environmental Protection Agency), aromatic compounds account for a significant proportion, among which 16 priority pollutants of PAHs are listed as the pollutants that have gained the concerned attention of the public in recent years. Li et al. (2003) sampled PAHs and conducted analysis of waste gases from the chimney flues of restaurant kitchens in southern Taiwan. Their results showed that mean Anthracene concentrations (gaseous phase + particulate phase) emitted from the stacks of ten restaurants: (i) four Chinese: concentration of 0.474–1.58 $\mu\text{g}/\text{Nm}^3$ (average value: 1.03 $\mu\text{g}/\text{Nm}^3$); (ii) two Western: concentration of 0.454–1.85 $\mu\text{g}/\text{Nm}^3$ (average value: 1.15 $\mu\text{g}/\text{Nm}^3$); (iii) two Fast food: concentration of 0.189–0.261 $\mu\text{g}/\text{Nm}^3$ (average value: 0.225 $\mu\text{g}/\text{Nm}^3$); and (iv) two Japanese: concentration of 0.191–0.266 $\mu\text{g}/\text{Nm}^3$ (average value: 0.225 $\mu\text{g}/\text{Nm}^3$) [4].

Anthracene (chemical formula of $\text{C}_{14}\text{H}_{10}$, Ant) is a tricyclic aromatic hydrocarbon derived from coal tar; melts at 218°C, boils at 354°C, insoluble in water but is soluble in most organic solvents such as carbon disulfide, alcohols, benzene, chloroform, and hydronaphthalenes [5]. Its molecular structure consists of three benzenelike rings joined side by side and its oxidation yields anthraquinone, the parent substance of a large class of dyes and pigments [6]. The Ant is one of a number of PAHs on EPA's priority pollutant list. Therefore, it is important to understand the influences of atmospheric plasma reactor for treating cooking fumes on Ant emission, special in the field of the air pollution control application.

Computational Fluid Dynamics (CFD) is a discipline that encompasses the numerical solution of the equations of motion (mass, momentum and energy) in a flow geometry of interest, together with subsidiary sets of equations reflecting the problem at hand [7]. Recently, CFD models are powerful predictive tools in combustion research and they have been widely used to simulate combustion in coal-fired power stations. Zhang and Zhao

(2007) demonstrated that the simulation and health risk assessment of residential particle pollution by coal combustion in China. Their study indicated that based on the simulated results, an engineering-oriented method was demonstrated to be effective in assessing indoor particle pollution by coal combustion and its health effect [8]. Khoshhal *et al.*, (2011) presented CFD study on influence of fuel temperature on NO_x emission in a HiTAC furnace. Their result indicated that the comparison between the predicted results and measured values have shown good agreement, which implies that the adopted combustion and NO_x formation models are suitable for predicting the characteristics of the flow, combustion, heat transfer, and NO_x emissions in the HiTAC chamber [9]. Lee *et al.*, (2011) shown that the use of the combined CFD and chemical reactor networks (CRN) approach has the ability to accurately predict NO_x emissions for lean-premixed combustion applications. Their predicted results agree reasonably well with the experimental data obtained from a simplified test combustor for the GE7FA gas turbine[10].

The main aim of this work is to investigate the combustion characteristics and pollutant decomposition of gaseous anthracene combustion in a model atmospheric plasma reactor and to compare combustion model predictions with experimental results for model validations. Although the flow is turbulent, the predictions for the flow field and combustion characteristics such as temperature distributions and gas concentrations are in good agreement with existing experimental data.

2. Experimental Method

2.1. Reaction system

A schematic diagram of the reaction system is sketched in Fig. 1. During simulation, the atmospheric plasma reactor size and operating parameters were taken from the self-designed atmospheric plasma reactor in our previous study [11-14]. Experimental data of temperature and anthracene concentration in an atmospheric plasma reactor for treating cooking fumes from Chang *et al.* [13] was used to validate the numerical model. Fig. 2 schematically showed the computational geometry of the atmospheric plasma reactor. The geometry of the torch used in numerical simulations is similar to that used in experiments. Number of calculation cells inside the computational domain is 490,300. The computation domain and meshing have been created by Gambit (2.4.6. version).

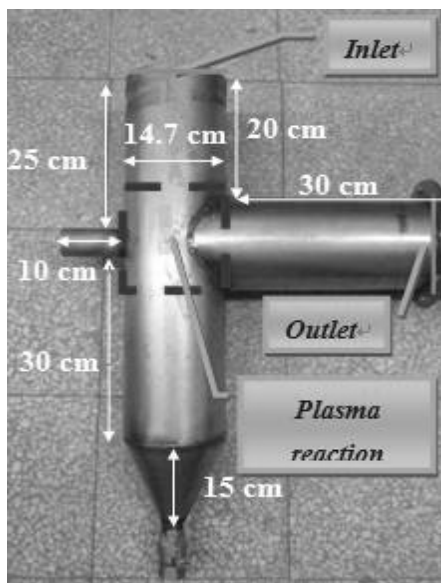


Figure 1. A full-scale reactor.

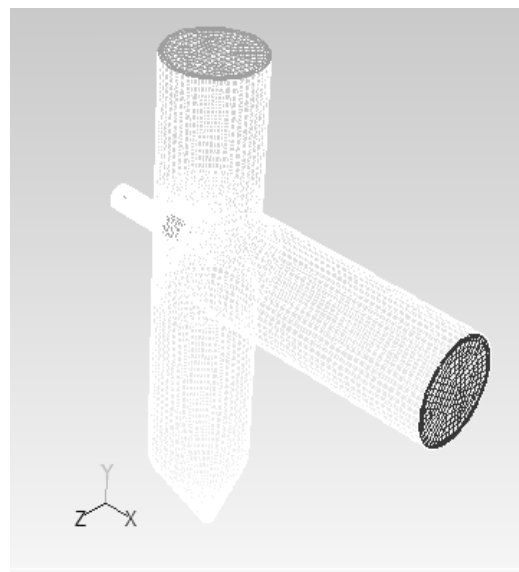


Figure 2. Schematic of the grid system.

2.2 Experimental methods and steps

The settings of boundary conditions in this study are shown in the following steps:

(a) Inlet: Initial calculation is conducted to simulate the process of the anthracene compounds of fugitive cooking fumes entering the torch reaction area under atmospheric pressure. The boundary conditions of the velocity inlet are obtained here.

(b) Outlet: At the outlet, the process of cooking fume enter the airspace after passing through the torch reaction area under atmospheric pressure plasma is simulated, and the pressure outlet is applied.

(c) The discharge pipes are made of stainless steel. Therefore, “steel” is chosen as the Fluent parameter, and the pipe thickness is set to 3 mm.

2.3 Models description

CFD modeling provides the visualization and interpretation of the atmospheric plasma reactor flow and reaction space. In this study, species transport model, chemical reactions, a volumetric reaction-based model with the eddy dissipation concept (EDC) model was used [15]. The governing equations to simulate the atmospheric plasma reactor are solved by using SIMPLE algorithm incorporated in commercial CFD software ANSYS FLUENT 12.1. This model is able to predict high temperature air combustion conditions [16, 17].

2.4 Chemical mechanism

In the chemical mechanism, the decomposition of anthracene molecules occur pathway. The pathway, originally investigated by DeCoster *et al.*, (2011), corresponds to the yields of major gas products (CO , CO_2 and O_2) and light hydrocarbons. Acetylene was the most abundant light hydrocarbon, followed by methane, ethylene, benzene, propylene and ethyl acetylene. Prevalent polycyclic aromatic compounds included fluorene-9-one, 9,10-anthracenedione, biphenylene, dibenzofuran, fluorene, indene, naphthalene, anthrone, xanthone and 2 naphthalenecarboxaldehyde [5].

3. Results and Discussion

In order to define the different relative distances used in CFD simulation, we can represent the different target position in the plasma reactor in a simple diagram as Figure 3. If we assume that a box (ABCD volume) is the main plasma reaction of activity, then the shading in the rectangle (that is, the ABCD section) designates the plasma reaction zone in the reactor. The reactant species enter into the AB-section, then pass the plasma torch, and through the BC-section to the vent of exit. Moreover, Figure 3 is the simulation of distribution of grid points (XY section) of treating anthracene with plasma torches. For convenience of discussion, the observation range of plasma reaction area is set within the region of an ABCD rectangle. The torch position of FLUENT simulated plasma is set as the origin (0, 0), the semi-diameter of circular tube within the system is 7.35 cm, and the distance between torch position and outlet end is 37.35 cm.

The calculation results are compared with the experimental data from the real plasma reactor in our lab. The measured volume flows, temperatures, and anthracene compound in flue gas have been averaged over a quasi stationary period. Hence, even if some transient species are unknown, the application of a simplified comprehensive mechanism is always appropriate in environmental engineering practice over a long steady period. Thus, if only final anthracene emission levels are of interest, the presented simplified model for the calculation of anthracene from restaurant cooking activities offers an excellent alternative to time-consuming and computationally expensive comprehensive mechanisms.

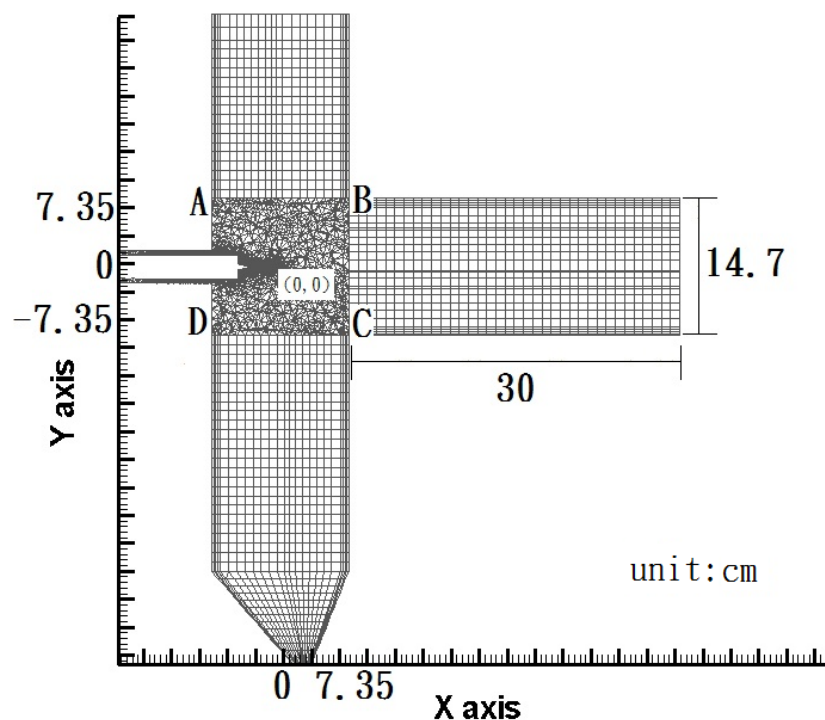


Figure 3. A description of grid relating to the atmospheric plasma reactor. (XY profile)



3.1 Temperature profiles

Gas temperature profiles in the atmospheric plasma reactor were obtained with a computational fluid dynamics code. When inputting plasma power at 24A, as shown in Figure 4, the highest temperature area in the flow field is in the central position of the plasma torches, of which temperature simulated value can reach 2243K. When leaving the reaction area, the temperature gradually decreases from the upstream to downstream, with the tail gases flowing to the outlet. The temperature tends to be accordant further to the right side, and for tail gas at the position of 37.35 cm, the temperature range is about 400K. With the increased distance, the heat energy efficiency progressively reduces, which results in a temperature drop.

3.2 Concentration profiles

The accuracy of CFD simulation depends on many factors. For example, the effects of appropriate geometry boundaries, the inlet turbulent parameters and the selected turbulence models (such as, low-Reynolds number $k-\epsilon$ model, renormalization group $k-\epsilon$ model or Shear Stress Transport $k-\omega$ model) are very important [18]. Based on the characteristic of plasma-torch, particular attention should be paid to the boundaries chosen for the plasma-reaction domain, because both the position of domain boundaries and the type of condition imposed (e.g., pressure node, velocity node, non-reflecting surface) are critical for the results of the modal analysis. Moreover, these limits are likely to be the same limits of the computational domain in the CFD simulation to be performed in the successive steps of the decomposition of anthracene compound in the atmospheric plasma reactor. The predicted levels of mass fraction of Ant progress variable on the horizontal axis (x-direction) or on the vertical symmetry plane near the plasma torch are shown in contour plots in Figure 5, respectively. In this study, the concentration of Ant in the inlet of duct was sampled and measured at 3.85×10^{-10} (mass fraction %). Based on this feeding level, the simulated removal efficiencies of Ant in the duct ranged from 37.1% to 47.1%, respectively.

4. Conclusion

In this study, the numerical simulation of decomposing anthracene compound in an atmospheric plasma reactor to treat cooking fume were carried out. The result obtained from our experimental was compared with the simulation data. The on-line measured temperature levels in the exhaust of reactor range from 300 to 400 K and they are similar to the simulation levels. The simulated removal efficiencies of Ant ranged from 37.1% to 47.1%, respectively. It was concluded that CFD methods can be used as a useful tool to assist the rational design of an atmospheric plasma reactor to treat cooking fume.

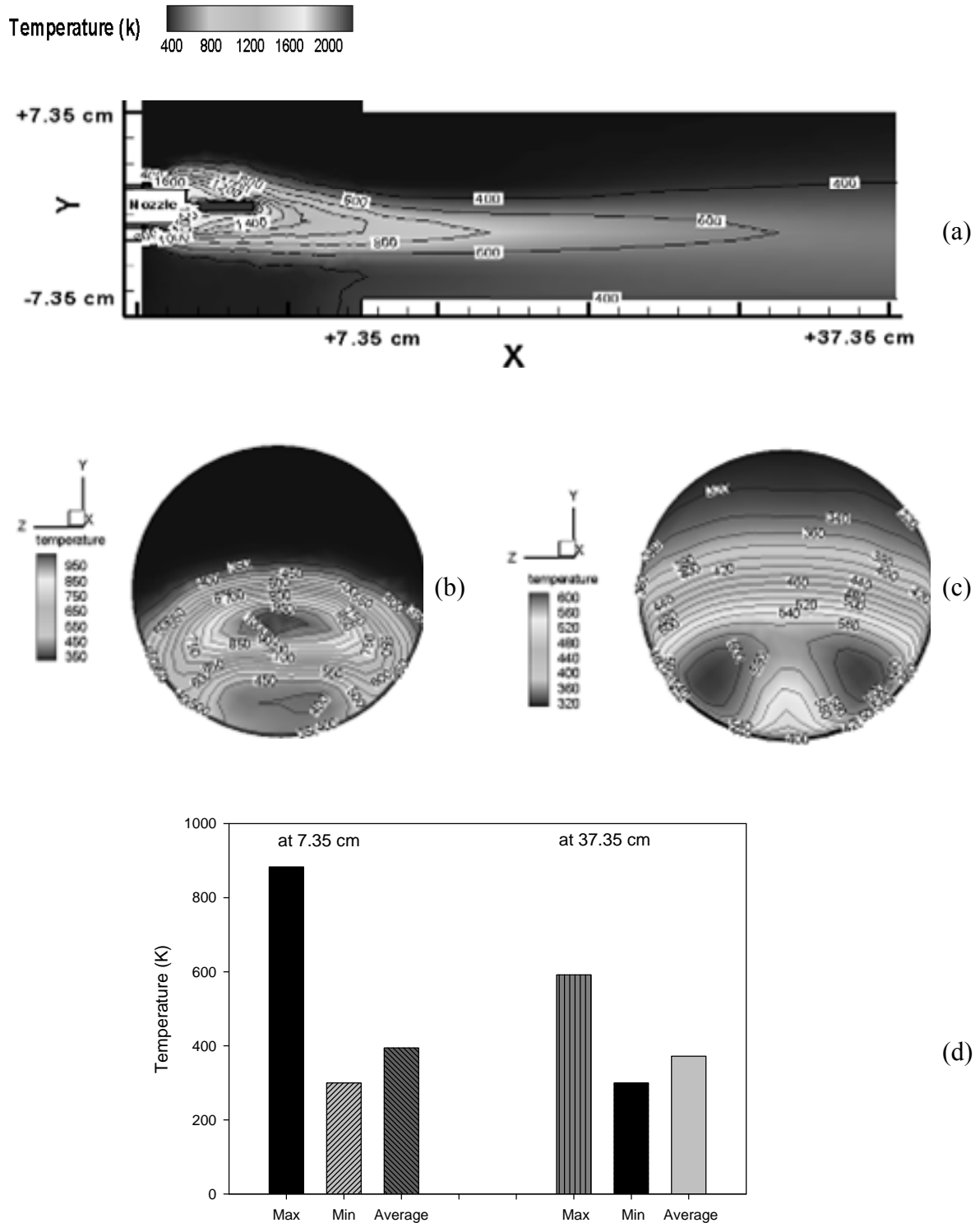


Figure 4. Temperature profiles (K): (a) at different X distances far from the center of plasma torch; (b-c) the distribution profile paralleled the BC-section at X= 7.35 (b) and X= 37.35 cm (c); (d) comparison of temperature levels between at X= 7.35 and X= 37.35 cm.

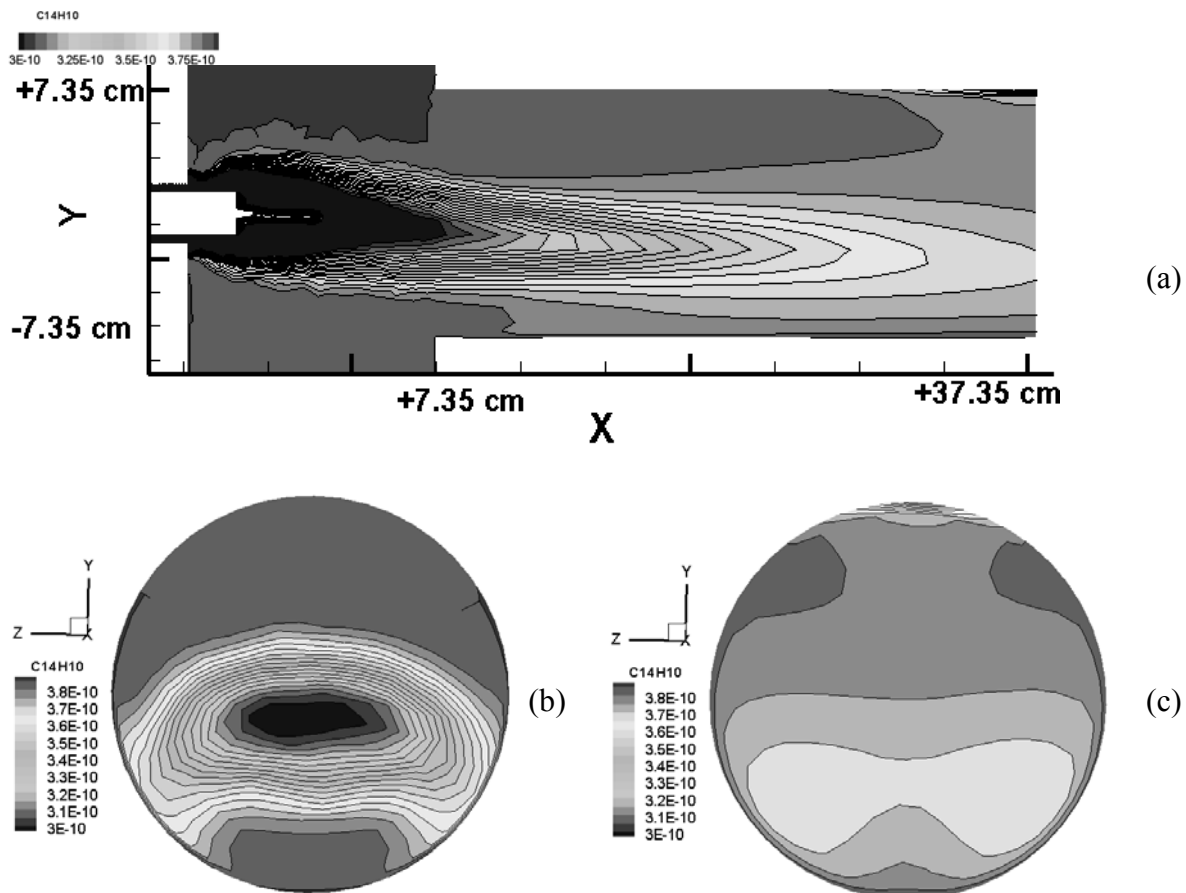


Figure 5. Concentration of anthracene profiles (%): (a) at different X distances far from the center of plasma torch; (b-c) the distribution profile paralleled the BC-section at X= 7.35 (b) and X= 37.35 cm (c).

Reference

- [1] Menzie, C. A., Potocki, B. B., and Santodonato, J. 1992. Exposure to Carcinogenic PAHs in the Environment. *Environmental Science & Technology*, 26: 1278–1284.
- [2] Chiang, T.A., Wu, P.F., Ko, Y.C. (1999). Identification of carcinogens in cooking oil fumes. *Environmental Research*, 81:18-22.
- [3] Li, C.T., Lin, Y.C., Lee, W.J. and Tsai, P.J., (2003). Emission of Polycyclic Aromatic Hydrocarbons and Their Carcinogenic Potencies from Cooking Sources to the Urban Atmosphere. *Environ. Health Perspect.* 111, 483-487.
- [4] Zhao, Y., Hu, M., Slanina, S. and Zhang, Y. (2007). Chemical Compositions of Fine Particulate Organic Matter Emitted from Chinese Cooking. *Environmental Science & Technology*, 41:99-105.
- [5] DeCoster, J., Ergut, A., Levensis, Y.A., Richter, H., Howard, J.B., and Carlson, J.B. 2007. PAH Emissions From High-Temperature Oxidation of Vaporized Anthracene. *Proceedings of the Combustion Institute*, 31: 491-499.
- [6] ANTHRACENE physical and chemical properties. *Chemicaland21.com* web site. <http://www.chemicaland21.com/industrialchem/organic/anthracene.htm> (updated : April 2, 2012)
- [7] Harris, C.K., Roekaerts, D., Rosendal, F.J.J., Buitendijk, F.G.J., Vreenegeer, A.J.N., Wang, H. 1996. *Computational Fluid Dynamics for Chemical Reactor Engineering*. *Chemical Engineering Science*, 51:1569-1594.
- [8] Zhang, Y. and Zhao, B. 2007. Simulation and health risk assessment of residential particle pollution by coal combustion in China. *Building and Environment*, 42: 614–622.
- [9] Khoshhal, A., Rahimi, M. and Alsairafi, A. A. 2011. CFD study on influence of fuel temperature on NOx emission in a HiTAC furnace. *International Communications in Heat and Mass Transfer*, 38 : 1421–1427.
- [10] Lee, D., Park, J., Jin, J. and Lee, M. 2011. A simulation for prediction of nitrogen oxide emissions in lean premixed combustor. *Journal of Mechanical Science and Technology* 25:1871-1878.
- [11] Hsieh L.T. 2007. Treatment of Cooking Oil Exhaust by the Application of Combining Atmospheric Plasma Technology and Enzyme Scrubbing. Final research project report. National Science Council of the Republic of



China, Taiwan. Grant #: NSC95-2211-E020-020.

[12] Hsieh, L.T. and Chang, H.C. 2010. Simulation of both temperature and velocity in the exhaust from an atmospheric plasma reactor for treatment the cooking fume. 2010 International Conference on Aerosol Science and Technology, Taipei, Taiwan, Sep. 24-25, 2010: 94-101.

[13] Chang, H.C., Mi, H.H., Lin, Y.C., Hsieh, L.T. and Chao, H.R. 2011. Removal of Gaseous Polycyclic Aromatic Hydrocarbons from Cooking Fumes Using an Atmospheric Plasma Reactor. *Journal of Environmental Science and Health Part A*, 46: 1443-1449.

[14] Hsieh, L.T., Chang, H.C. 2011. Preliminary study of numerical simulation of benz[a]anthracene compound in an atmospheric plasma reactor to treat cooking fume. 2011 International Conference on Aerosol Science and Technology, Tainan, Taiwan, Oct. 12-14, 2011: 268-269.

[15] Magnussen, B.F. 1981. On the structure of turbulence and a generalized eddy dissipation concept for chemical reaction in turbulent flow, *Proceeding of the Nineteenth AIAA Aerospace Science Meeting*, Missouri, USA.

[16] Orsino, S., Weber, R., Bollettini, U. 2001. Numerical simulation of combustion of natural gas with high-temperature air. *Combustion Science and Technology* 170: 1-34.

[17] Christo, F.C. and Dally, B.B. 2005. Modeling turbulent reacting jets issuing into a hot and diluted coflow. *Combustion and Flame* 142: 117-129.

[18] Rong, L., Elhadidi, B., Khalifa, H.E., Nielsen, P.V., Zhang, G. Validation of CFD simulation for ammonia emissions from an aqueous solution. *Computers and Electronics in Agriculture*. 2011: 261-271.